Raman-active phonons and Nd^{3+} crystal-field studies of weakly doped $Nd_{1-x}Sr_xMnO_3$

S. Jandl*
Département de Physique, Université de Sherbrooke, 2500 Boulevard Université, Sherbrooke J1K 2R1, Canada

A. A. Mukhin and V. Yu Ivanov
General Physics Institute of the Russian Academy of Sciences, 38 Vavilov St., 119991 Moscow, Russian Federation

V. Nekvasil
Institute of Physics, Czech Academy of Sciences, Cukrovarnická 10, CZ-162 53 Prague 6, Czech Republic

M. L. Sadowski
Grenoble High Magnetic Field Laboratory, 25, Avenue de Martyrs, Boîte Postale 166, F-38042 Grenoble, France
(Received 14 February 2005; revised manuscript received 12 April 2005; published 14 July 2005)

Raman-active phonons as a function of temperature and Nd^{3+} infrared active crystal-field excitations under high magnetic fields have been studied in $Nd_{0.975}Sr_{0.025}MnO_3$ and $Nd_{0.9}Sr_{0.1}MnO_3$ and compared to $NdMnO_3$ results. While long range antiferromagnetism disappears in $Nd_{0.9}Sr_{0.1}MnO_3$, low energy phonon softening and phase separation in domains develop as a result of doping. Calculation of g tensors indicates that additional crystal-field excitations observed in $Nd_{0.975}Sr_{0.025}MnO_3$ and $Nd_{0.9}Sr_{0.1}MnO_3$ are due to x-y twinning.

DOI: 10.1103/PhysRevB.72.024423 PACS number(s): 75.47.Lx, 78.30.Hv, 75.10.Dg

I. INTRODUCTION

Due to charge compensation, substitution of the rare earth ion R^{3+}, by a divalent cation A^{2+}, generates Mn^{4+} ions in $R_{1-x}A_xMnO_3$ (R=lanthanides and A=Ba, Sr, or Ca).While $RMnO_3$ compounds are antiferromagnetic with important Jahn-Teller distortions, lanthanide substitution leads to double exchange interactions, reduction of Jahn-Teller-type distortions and simultaneous observation of metallic and ferromagnetic character for $x \sim 0.3$.[1–3] Near the concomitant paramagnetic insulator-ferromagnetic metallic phase transition,[4] a colossal negative magnetoresistance, reflecting strong interconnections between the electrical and magnetic properties, has been observed. The Mn^{3+}/Mn^{4+} distribution modifies the Mn-O bond lengths and provokes structural disorder strongly temperature and doping dependent. The static or dynamical characters of the involved charge, lattice magnetic, and orbital degrees of freedom are still a debated issue.[5] The precursor effects expected in the low-doping regime are of great interest since they provide an insight to the physical parameters or mechanisms that play major roles even in the large-doping regime. Also, according to mean-field theory, the magnetic ground state corresponds to a canted antiferromagnetic homogeneous state at low-doping regime[6] while recent theoretical and experimental developments predict inhomogeneous ground state and phase separation.[7] Puzzling ferromagnetic insulating states, that the double exchange described by Zener[8] could not explain, have been reported in the low-doping regime for Ca- and Sr-doped $LaMnO_3$.[9] They were tentatively interpreted in terms of either polaron[10] or orbital ordering[11] underlining the important role of electron-phonon coupling.[12]

The Nd-based compounds have been less studied in comparison to the La compounds; they are nevertheless interesting since the strength of the double exchange interactions is weaker due to larger lattice distortions provoked by the smaller Nd^{3+} ions.[13] Consequently, in a doped system like $Nd_{1-x}(Ca,Sr)_xMnO_3$ as compared to $La_{1-x}(Ca,Sr)_xMnO_3$ a closer competition with generic instabilities, such as antiferromagnetic superexchange, orbital and charge ordering, would exist between the electron-phonon, electron-electron, and the double exchange interactions.[14] $NdMnO_3$, with its orthorhombic D_{2h}^{16}-*Pbnm* space group, may be viewed as a stacking of MnO_2-NdO layers along the c axis accompanied by tilts of the MnO_6 octahedra whereas three different pair lengths of Mn^{3+}-O^{2-} bonds are associated with coherent Jahn-Teller distortions. It is an insulator characterized by an antiferromagnetic low-temperature ground state and static Jahn-Teller distortions.[15] Neutron diffraction measurements suggest the coexistence of ferromagnetic and antiferromagnetic interactions resulting in canted-antiferromagnetic layered structure for the Mn subsystem;[16,17] the magnetic structure corresponds to a ferromagnetic exchange in the MnO_2 planes and an antiferromagnetic exchange between them. The Mn^{3+} spins order at $T_N \sim 75$ K and their moments saturate at ~ 20 K.[16] While no evidence for the Nd^{3+} ordering, down to 1.8 K, is reported in Ref. 16; the Nd sublattice orders in a ferromagnetic arrangement with the moments parallel to the c direction below $T \sim$ 13 K according to Ref. 17. A recent study of Raman active phonons in $NdMnO_3$ (Ref. 18) has indicated that the phonon frequencies, intensities, and bandwidths are sensitive to the magnetic evolution of the Mn^{3+} sublattice as a function of temperature with no particular indication for Nd^{3+} sudden moment ordering. In particular, similarly to orthorhombic $LaMnO_3$, the $NdMnO_3$ structure is distorted by a static Jahn-Teller effect consistent with the D_{2h}^{16} group and the most intense ~ 601 cm^{-1} Raman active B_{1g} phonon in *Pbnm* notation (B_{2g} phonon in *Pnma* notation) softens below $T_N \sim$ 75 K following the paramagnetic to canted-antiferromagnetic phase transition.

A phase diagram of $La_{1-x}Sr_xMnO_3$ has been reported for $x \leqslant 0.2$. A canted-antiferromagnetic ground state, was ob-

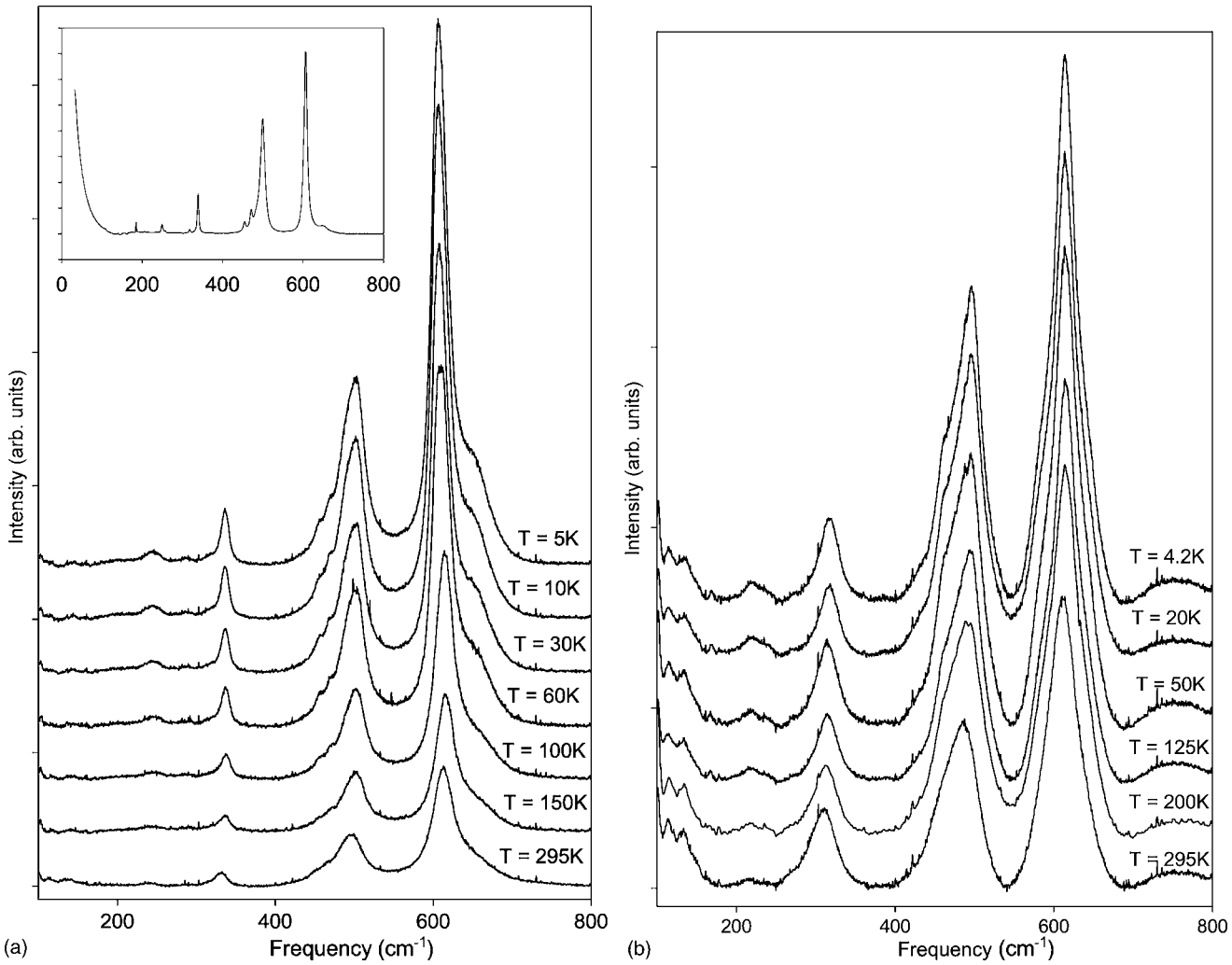

FIG. 1. (a) $Nd_{0.975}Sr_{0.025}MnO_3$ A_{1g} and B_{1g} Raman-active phonons as a function of temperature. Inset: $NdMnO_3$ Raman-active phonons at 5 K. (b) $Nd_{0.9}Sr_{0.1}MnO_3$ A_{1g} and B_{1g} Raman-active phonons as a function of temperature.

served for $x<0.1$, and a ferromagnetic insulator ground state was detected for $0.1\leqslant x\leqslant 0.15$.[19] While the phase diagram seems similar in the case of $Nd_{1-x}Sr_xMnO_3$,[20] magnetic phase separation was invoked in the case of low-doped $Nd_{1-x}Ca_xMnO_3$ ($x\leqslant 0.15$).[21]

In high-temperature superconducting cuprates and their parent compounds, infrared transmission technique has been used successfully for the study of rare-earth crystal-field (CF) excitations.[22–24] In these materials, and similarly to the manganites, the magnetism plays a major role and the electrons are strongly correlated. For instance Nd^{3+} and Pr^{3+} CF excitations have allowed the study of oxygen nonstoichiometry, cerium doping effects and stripes formation.[25–27] In spite of the interesting informations, concerning the local inhomogeneities, electronic and magnetic properties, that provide the rare earth ion CF excitation studies, these have been limited in the manganites to the study of $NdMnO_3$ (Nd^{3+} ion) ground state Kramers doublet (KD) splitting[28] and its ${}^4I_{9/2}\rightarrow {}^4I_{11/2}$, ${}^4I_{13/2}$ CF transitions under magnetic field.[29]

In the case of $La_{1-x}A_xMnO_3$, Raman spectroscopy has proved its efficiency in characterizing the Jahn–Teller distortions and the mixed valence manganites disorder,[30] allowing monitoring of the dopings at microscopic levels. In addition, nanoscale phase separation, defects, and nonstochiometry should manifest, in the detected doped manganites rare earth CF excitations, regardless of the widespread belief that optical techniques are not appropriate to study rare-earth electronic *f-f* transitions in opaque materials.[31]

We have succeeded recently in calculating the 15 CF Hamiltonian parameters of $NdMnO_3$ using 19 measured CF levels, energies of Kramers doublet exchange splittings, the x components of g tensors, *ab initio* methods and an appropriate superposition model.[29] The task was complicated by the Nd^{3+} ions C_s site symmetry and by the lack of CF data in similar structures. A way to validate the $NdMnO_3$ CF calculations is to verify the predictions of the g tensors along the crystallographic axis y, by a comparison with experimental Kramers doublet splittings, in lightly doped $NdMnO_3$.

In this paper we present a study of $Nd_{1-x}Sr_xMnO_3$ Raman-active phonons and CF excitations for $x=0.025$ and $x=0.1$, by combining the Raman scattering technique with the infrared transmission measurements. The objectives are to determine (i) if antiferromagnetism persists at low Sr dop-

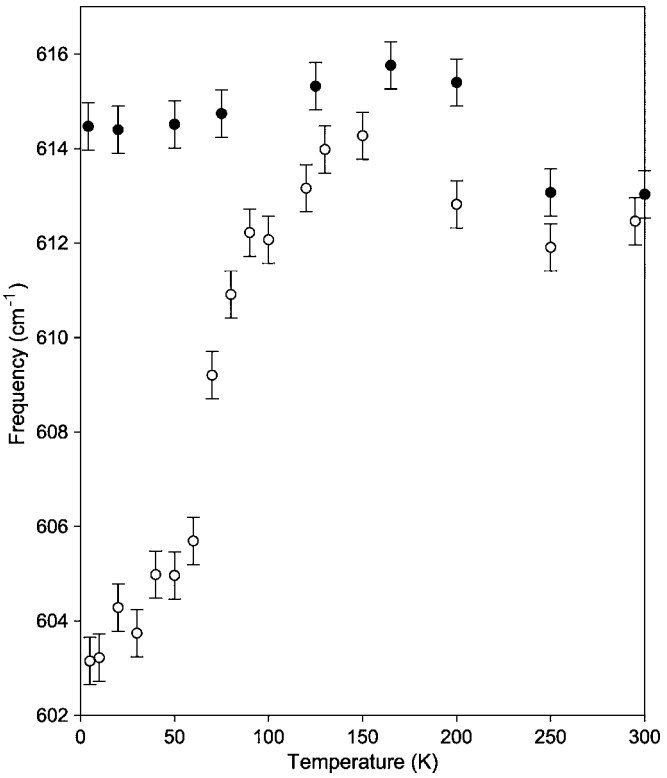

FIG. 2. Temperature evolution of the 612 cm^{-1} B_{1g} phonon frequency in $Nd_{0.975}Sr_{0.025}MnO_3$ (white circles), and $Nd_{0.9}Sr_{0.1}MnO_3$ (black circles).

ing, (ii) if the local structure is affected by defects or phase separation and differs from the averaged one, (iii) if the Hamiltonian CF parameters of $NdMnO_3$ describe the magnetic data including the Zeeman splittings of the Nd^{3+} Kramers doublets in the doped compounds.

II. EXPERIMENTS

The $Nd_{1-x}Sr_xMnO_3$ ($x=0.025$ and 0.1) single crystals ($\sim$1, 2 mm, 200 μm) were grown by the floating zone method as described in Ref. 32. 0.5 cm^{-1} resolution Raman spectra were measured in the backscattering configuration using a He-Ne laser (632.8 nm) and a Labram-800 Raman microscope spectrometer equipped with $\times 50$ objective, appropriate notch filter and nitrogen cooled charge coupled device (CCD) detector. The samples were mounted on the cold finger of a microhelium Janis cryostat with the z axis ($D_{2h}^{16}-Pbnm$ setting) parallel to the incident radiation and the laser power was kept at 0.2 mW to avoid local heating. No analyzer was used, so that both $xx(A_{1g})$ and $xy(B_{1g})$ configurations become accessible. Absence of spurious signals was verified by the reproducibility of the spectra and their corresponding selection rules.

The infrared transmission measurements as a function of temperature were obtained in the 1800–5000 cm^{-1} range with a Fourier transform interferometer BOMEM DA3.002 equipped with an InSb detector, quartz-halogen and globar sources, and a CaF_2 beam splitter. For measurements under magnetic fields up to 13 T, with 1 cm^{-1} resolution, a Bruker

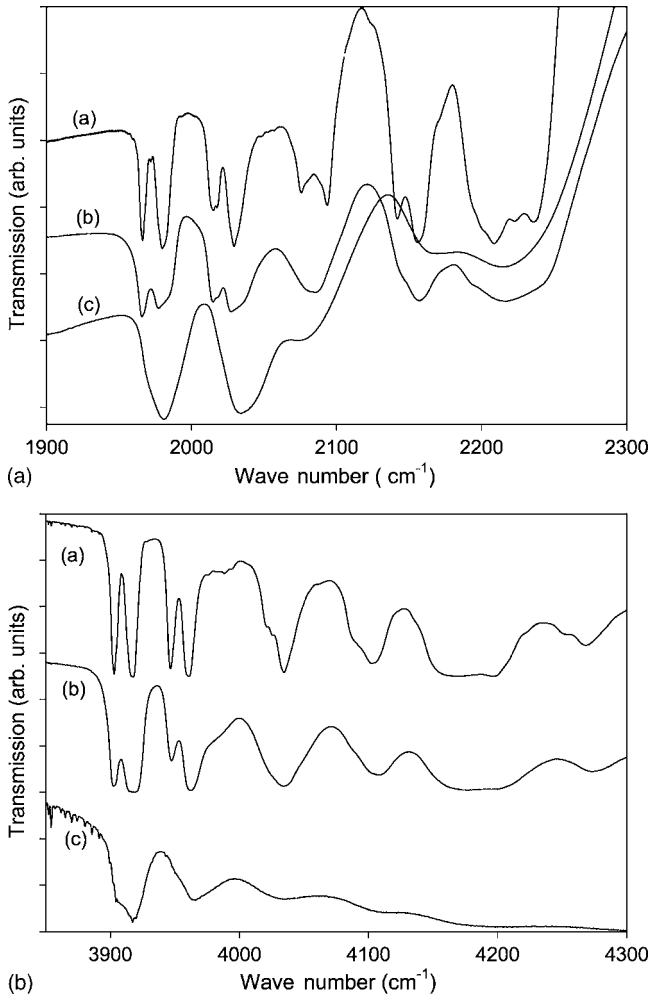

FIG. 3. (a) ${}^4I_{9/2} \rightarrow {}^4I_{11/2}$ CF transitions at $T=8$ K in (a) $NdMnO_3$, (b) $Nd_{0.975}Sr_{0.025}MnO_3$, and (c) $Nd_{0.9}Sr_{0.1}MnO_3$. (b) ${}^4I_{9/2} \rightarrow {}^4I_{13/2}$ CF transitions at $T=8$ K in (a) $NdMnO_3$, (b) $Nd_{0.975}Sr_{0.025}MnO_3$, and (c) $Nd_{0.9}Sr_{0.1}MnO_3$.

Instruments model 113 Fourier transform spectrometer, equipped with tungsten and globar light sources, was used to collect and analyze the spectra. The samples were placed in the bore of a superconducting magnet and in a helium bath cryostat at 1.8 K, with the magnetic field and the incident radiation parallel to the x axis. A composite Si bolometer mounted directly beneath the sample was used to measure the intensity of the transmitted light.

III. RESULTS AND DISCUSSION

Sixty phonon modes are associated with the Γ point of orthorhombic $NdMnO_3$ space group $D_{2h}^{16}-Pbnm$. Twenty-four of them ($7A_g+7B_{1g}+5B_{2g}+5B_{3g}$) are Raman active.[33] In Figs. 1(a) and 1(b) Raman spectra of $Nd_{0.975}Sr_{0.025}MnO_3$ and $Nd_{0.9}Sr_{0.1}MnO_3$, as a function of temperature, are presented, respectively. Both A_g and B_{1g} phonons, of stretching and bending types, related to octahedral distortions ($\sim$600–500 cm^{-1}) and octahedral tilting ($\sim$300 cm^{-1}) are detected, whereas broadbands due to large noncoherent Jahn-Teller distortions resulting in disordered-induced phonon

TABLE I. $^4I_{11/2}$ and $^4I_{13/2}$ experimental $Nd_{1-x}Sr_xMnO_3$ CF energy levels and the absolute values of the Kramers doublet g_y tensor of Nd^{3+}. $|g_y|$ (calc.) corresponds to the $NdMnO_3$ CF Hamiltonian predictions.

		$Nd_{0.975}Sr_{0.025}MnO_3$		$Nd_{0.9}Sr_{0.1}MnO_3$			
CF level	$NdMnO_3$	Site I	Site II	Site I	Site II	$\|g_y\|$ (Calc.)	$\|g_y\|$ (Exp.)
$^4I_{11/2}$	1973	1978	1986	1983	1992	0.5	0.45
	2022	2027	2035	2037	2046	2.3	2.1
$^4I_{13/2}$	3910	3914	3922	3916	3924	0.1	
	3948	3959	3965	3964	3976	1.2	

density of states[34] are absent. This indicates the overall persistence of coherent Jahn-Teller distortions at low Sr doping. In contrast to $La_{0.9}Sr_{0.1}MnO_3$,[35] no band ($\sim$420 cm^{-1}) indicative of a rhombohedral phase is detected in $Nd_{0.9}Sr_{0.1}MnO_3$ and the 615 cm^{-1} phonon intensity, that weakens in $La_{0.9}Sr_{0.1}MnO_3$ below (T_C=200 K),[35] remains strong at low temperature excluding long range ferromagnetism. Actually, phonon intensities are strongly reinforced below T_N=75 K in $NdMnO_3$ (Ref. 18) and the same trend is observed in $Nd_{0.975}Sr_{0.025}MnO_3$ while less pronounced in $Nd_{0.9}Sr_{0.1}MnO_3$ [Figs. 1(a) and 1(b)]. The phonon frequencies as measured at T=4.2 K ($\sim$603,499,483,468,334, 243 cm^{-1} for $Nd_{0.975}Sr_{0.025}MnO_3$ and $\sim$615,498,468,319, 220 cm^{-1} for $Nd_{0.9}Sr_{0.1}MnO_3$) are comparable to $NdMnO_3$'s A_g(495,468,335,245 cm^{-1}) and B_{1g} (602,482 cm^{-1}) phonons.[18] Nevertheless, the phonon widths in the doped samples are broadened indicating some local disorder and small distortions affecting mainly the phonon lifetime; e.g., 17 and 23 cm^{-1} for the 602 cm^{-1} phonon in $Nd_{0.975}Sr_{0.025}MnO_3$ and $Nd_{0.9}Sr_{0.1}MnO_3$, respectively, as compared to 7 cm^{-1} in $NdMnO_3$. The two low energy A_{1g} phonon frequencies (335 and 245 cm^{-1} in $NdMnO_3$) are particularly affected by doping. They correspond to the vibration of the Nd/Sr ions with respect to the MnO_6 octahedra and they downshift to 334,243 and 319,220 cm^{-1} in $Nd_{0.975}Sr_{0.025}MnO_3$ and $Nd_{0.9}Sr_{0.1}MnO_3$, respectively. Softening of the 236 cm^{-1} A_{1g} mode in rhombohedral $LaMnO_3$ has been associated with the occurrence of distortions,[36] and similarly to the $La_{1-x}Sr_xMnO_3$ system[37] the frequency shifts have the opposite sign to what might be predicted from the atomic masses of Nd (144) and Sr (88) in the mixed crystals.[38] A decrease of the force constants in the Sr doped sample lowers the phonon frequencies and reflects the sensitivity of the Mn-*d* orbital and O-*p* orbital overlap to the internal pressure generated by the Nd/Sr sites.[39]

Softening of the 607 cm^{-1} phonon below $\sim T_N$=75 K observed in $NdMnO_3$ and $Nd_{0.975}Sr_{0.025}MnO_3$ disappears in $Nd_{0.9}Sr_{0.1}MnO_3$ (Fig. 2). In contrast to spin echo measurements which infer anomalous softening of bending modes around 450–482 cm^{-1},[40] Sr doping reduces the Jahn-Teller distortions and tends to suppress the phonon softenings. Granado *et al.*[41] have studied $La_{1-x}Mn_{1-x}O_3$ samples and have observed the softening of the $\sim$610 cm^{-1} Raman-active phonon. By scaling the frequency shift to the normalized square of the sublattice magnetization, they have associated such softening with spin-phonon coupling caused by phonon modulation of the nearest neighbors exchange integral. They have also shown that the magnetically induced changes in the lattice parameters, which remain minor, have no significant influence. Recent theoretical studies have proposed that phonon softening could be triggered by increasing the Jahn-Teller interaction that favors its mixing with orbital excitation[42,43] and resonant x-ray scattering has suggested that spin and orbital degrees of freedom are coupled.[44] Absence of softening in $Nd_{0.9}Sr_{0.1}MnO_3$ reflects the vanishing of long range antiferromagnetism. Hence, study of the Raman-active phonons of $Nd_{1-x}Sr_xMnO_3$ indicates that Sr low doping generates local defects without affecting the overall coherent Jahn–Teller distortions. While long range antiferromagnetism persists in $Nd_{0.975}Sr_{0.025}MnO_3$, it is suppressed in $Nd_{0.9}Sr_{0.1}MnO_3$. In contrast to $La_{0.9}Sr_{0.1}MnO_3$, no long range ferromagnetism is observed in $Nd_{0.9}Sr_{0.1}MnO_3$.

Presence of magnetic domains, on a short scale in a phase separated sample, should affect locally the CF excitations by lifting the Nd^{3+} KD degeneracy. If the $Nd_{1-x}Sr_xMnO_3$ structures were ideal perovskite, the Nd^{3+} ions would have occupied centrosymmetrical sites preventing the CF excitations from being infrared active. The Jahn-Teller distortions lower the Nd^{3+} site point group symmetry rendering the CF excitations magnetic/electric dipole allowed. In the low Sr doped $NdMnO_3$, the relative static and coherent character of the Jahn–Teller distortions counters excessive broadening of the CF transitions as confirmed by the Raman active phonon widths.

In Figs. 3(a) and 3(b), $^4I_{9/2} \rightarrow {}^4I_{11/2}$ and $^4I_{9/2} \rightarrow {}^4I_{13/2}$ Nd^{3+} CF transitions at T=8 K are presented for $NdMnO_3$, $Nd_{0.975}Sr_{0.025}MnO_3$, and $Nd_{0.9}Sr_{0.1}MnO_3$. The expected six ($^4I_{11/2}$) and seven ($^4I_{13/2}$) CF levels are observed in the 1950–2250 and 3900–4300 cm^{-1} ranges, respectively. At T=8 K the degeneracy of the KD ground state is lifted in $NdMnO_3$ as well as in $Nd_{0.975}Sr_{0.025}MnO_3$ and $Nd_{0.9}Sr_{0.1}MnO_3$. This lifting of degeneracy ($\sim$14 cm^{-1} in $NdMnO_3$, $\sim$12 cm^{-1} in $Nd_{0.975}Sr_{0.025}MnO_3$, and $\sim$10 cm^{-1} in $Nd_{0.9}Sr_{0.1}MnO_3$), which is not masked by absorption band broadenings due to distortions generated by the Jahn-Teller effect and the MnO_6 octahedra rotation, is observed in the three compounds as obtained by the first $^4I_{11/2}$ and $^4I_{13/2}$ two levels absorption band fittings (site I in Table I). The $NdMnO_3$ CF Hamiltonian of Ref. 29 predicts adequately, within the CF parameters mean error, site I CF levels in $Nd_{0.975}Sr_{0.025}MnO_3$ and $Nd_{0.9}Sr_{0.1}MnO_3$. This indicates that even in $Nd_{0.9}Sr_{0.1}MnO_3$ there are regions where antiferromagnetism is not suppressed. In addition to the Nd^{3+} sites as

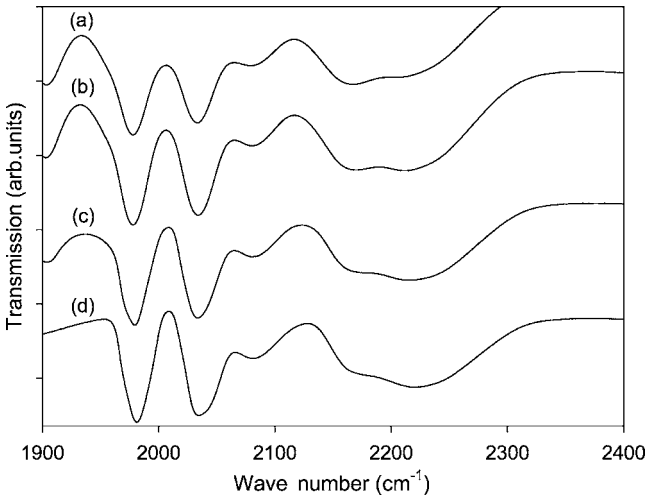

FIG. 4. $Nd_{0.9}Sr_{0.1}MnO_3$ $^4I_{9/2} \rightarrow {}^4I_{11/2}$ CF transitions as a function of temperature. (a) 150, (b) 100, (c) 50, (d) 9 K.

observed in $NdMnO_3$, additional CF excitations that could be associated with ferromagnetic domains are obtained in the doped samples by fitting the absorption bands (site II in Table I). Widths of the levels between 150 and 9 K are not temperature dependent as exemplified by $Nd_{0.9}Sr_{0.1}MnO_3$ (Fig. 4); they are mainly provoked by local distortions that persist with no significant modifications at low temperature. At $T=1.8$ K, the low energy excited multiplet KD components disappear following the depletion of the ground state excited level KD [Fig. 5(a)] rendering the observation of the CF excitations more accurate. While Sr doping broadens the CF excitations (9, 18, and 20 cm^{-1} in the 1983 cm^{-1} level case and 13,23,24 cm^{-1} in the 2031 cm^{-1} level case for $x=0$, 0.025, and 0.1, respectively, [Fig. 3(a)]; it does not produce new CF excitations shifted by few 10 cm^{-1} as generated by apical oxygens and observed in the case of cerium-doped Pr_2CuO_4 (Ref. 26) and Nd_2CuO_4.[27] This indicates that, in contrast to the high T_c cuprates, oxygen stoichiometry is not affected by doping and that the $Mn^{3+}\backslash Mn^{4+}$ mixed valence insures complete charge compensation. Under applied magnetic field, Zeeman splittings of two Nd^{3+} nonequivalent sites are observed [stars and arrows of Figs. 5(b) and 5(c)]. One of the sites has been reported in a previous untwined $NdMnO_3$ CF study for which the g_x tensors have been evaluated.[29] The CF excitations indicated with arrows in Figs. 5(b) and 5(c), (1971–2000 cm^{-1}); (2022–2049 cm^{-1}) under $B=8$ T and (1968–2012 cm^{-1}); (2019–2059) under $B=12$ T, correspond to a magnetic field applied parallel to the x axis with $g_x=5.2$ and 4.8 for the two $^4I_{11/2}$ lowest levels, respectively, in agreement with Ref. 29. In order to determine the origin of the additional Nd^{3+} site, we have calculated the g_y tensors using the CF parameters of Ref. 29 and measured the CF excitations of a twinned $NdMnO_3$ sample.

$g_y=0.5$ and 2.3 were obtained for the two $^4I_{11/2}$ lowest levels, respectively. For the magnetic field applied parallel to the y axis their predicted splitting would be (2.7 cm^{-1}), (12.5 cm^{-1}) for $B=8$ T and (4.1 cm^{-1}), (18.8 cm^{-1}) for $B=12$ T. The observed splittings of the two $^4I_{11/2}$ lowest levels

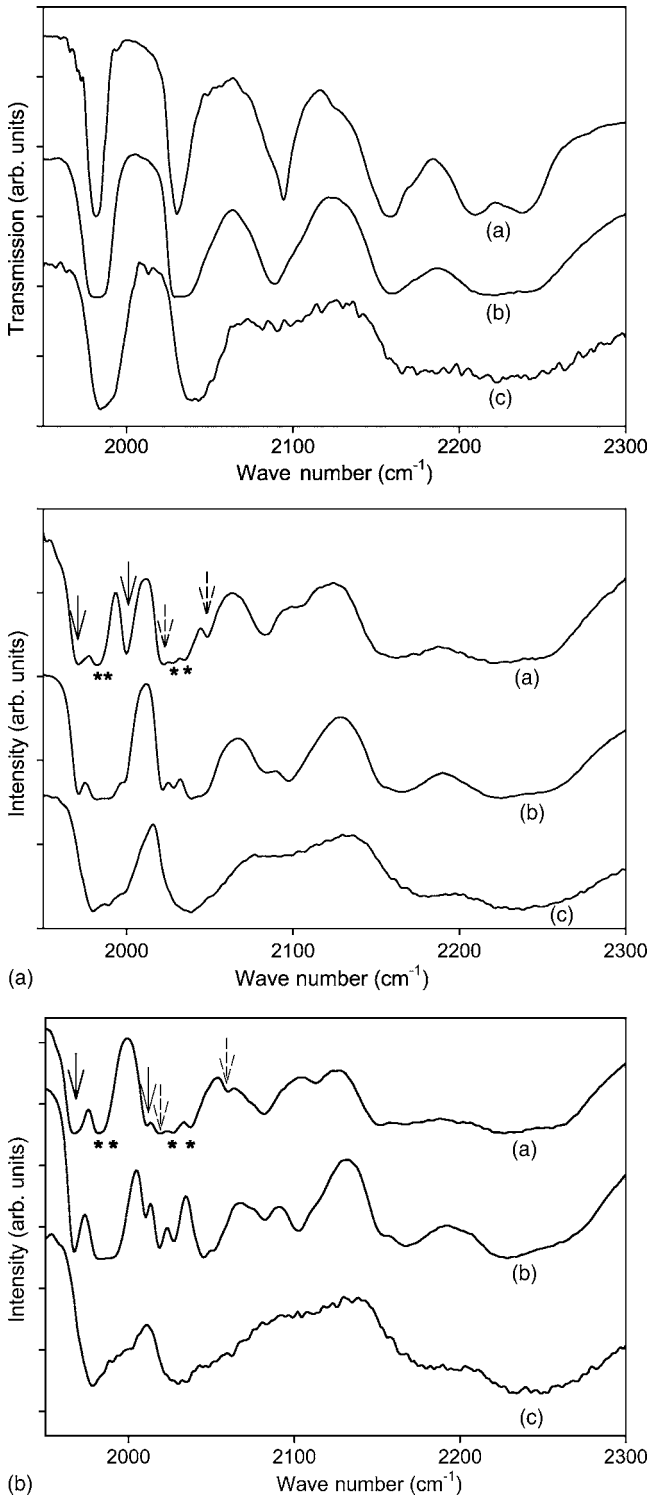

FIG. 5. (a) $^4I_{9/2} \rightarrow {}^4I_{11/2}$ CF transitions at $T=1.8$ K in (a) $NdMnO_3$, (b) $Nd_{0.975}Sr_{0.025}MnO_3$, and (c) $Nd_{0.9}Sr_{0.1}MnO_3$. (b) $^4I_{9/2} \rightarrow {}^4I_{11/2}$ CF transitions under applied magnetic field $B=8$ T at $T=1.8$ K in (a) $NdMnO_3$, (b) $Nd_{0.975}Sr_{0.025}MnO_3$, and (c) $Nd_{0.9}Sr_{0.1}MnO_3$. ↓ and * indicate the splittings associated with the g_x and g_y tensors, respectively. (c) $^4I_{9/2} \rightarrow {}^4I_{11/2}$ CF transitions under applied magnetic field $B=12$ T at $T=1.8$ K in (a) $NdMnO_3$, (b) $Nd_{0.975}Sr_{0.025}MnO_3$, and (c) $Nd_{0.9}Sr_{0.1}MnO_3$. ↓ and * indicate the splittings associated with the g_x and g_y tensors, respectively.

in the twinned $NdMnO_3$ sample as indicated with stars in Figs. 5(b) and 5(c) are in good agreement with the predictions ($\sim 3\ cm^{-1}$),($\sim 11\ cm^{-1}$) for $B=8$ T and ($\sim 4.1\ cm^{-1}$), ($\sim 17\ cm^{-1}$) for $B=12$ T. The CF excitations of $Nd_{0.975}Sr_{0.025}MnO_3$ and $Nd_{0.9}Sr_{0.1}MnO_3$, even though less resolved than in $NdMnO_3$ under applied magnetic field, coincide with those of twinned $NdMnO_3$ indicating that twinning characterizes Sr-doped $NdMnO_3$.

IV. CONCLUSION

Study of the $Nd_{1-x}Sr_xMnO_3$ ($x=0.05$ and 0.1) single crystals Raman-active phonons indicates that in spite of local disorder that broadens the phonon bands, the coherent Jahn-Teller distortions persist. No phonon bands that could be related to long range ferromagnetism are observed in the doped samples while long range antiferromagnetism vanishes in $Nd_{0.9}Sr_{0.1}MnO_3$. Sr doping provokes softening of low frequencies A_{1g} phonons reflecting force constants renormalization.

The CF excitations of $Nd_{1-x}Sr_xMnO_3$ indicate that oxygen stoichiometry is not affected by Sr doping. A site develops with Sr doping revealing phase separation between antiferromagnetic and possible ferromagnetic domains. The validity of the CF parameters calculated for $NdMnO_3$ has been confirmed by fitting the CF excitations observed in a twinned $NdMnO_3$ sample. Such *x*-*y* axes twinning characterizes the $Nd_{1-x}Sr_xMnO_3$ ($x=0.05$ and 0.1) single crystals.

ACKNOWLEDGMENTS

The authors would like to thank A. M. Balbashov for the samples growth. S.J. acknowledges support from the National Science and Engineering Research Council of Canada and the Fonds Québécois de la Recherche sur la Nature et les Technologies. Also gratefully acknowledged is the Grant Agency of the Czech Republic for its Grant No. 202/03/0552. The work in Prague was also supported by the Institutional Project No. AV0Z1-010-91. This work was supported in part by the Russian Foundation for Basic Researches (03-02-16759) and the Quantum Macrophysics Program of the Russian Academy of Sciences.

*Electronic address: serge.jandl@usherbrooke.ca

[1] C. Zener, Phys. Rev. **82**, 403 (1951).
[2] S. Jim, T. H. Tiefel, M. McCormack, R. Fastnacht, R. Ramesh, and L. H. Chen, Science **264**, 413 (1994).
[3] D. I. Khomskii and G. A. Sawatzky, Solid State Commun. **102**, 87 (1997).
[4] J. M. D. Coey, M. Viret, and S. von Molnar, Adv. Phys. **48**, 167 (1999).
[5] Y. Tokura and N. Nagaosa, Science **288**, 462 (2000).
[6] P. G. de Gennes, Phys. Rev. **118**, 141 (1960).
[7] A. Moreo, S. Yunoki, and E. Dagotto, Science **283**, 2034 (1999).
[8] C. Zener, Phys. Rev. **82**, 403 (1951).
[9] Y. Yamada, J. Suzuki, K. Oikawa, S. Katano, and J. A. Fernandez-Baca, Phys. Rev. B **62**, 11600 (2000).
[10] Y. Yamada, O. Hino, S. Nohdo, R. Kanao, T. Inami, and S. Katano, Phys. Rev. Lett. **77**, 904 (1996).
[11] Y. Endoh, K. Hirota, S. Ishihara, S. Okamoto, Y. Murakami, A. Nishizawa, T. Fukuda, H. Kimura, H. Nojiri, K. Kaneko, and S. Maekawa, Phys. Rev. Lett. **82**, 4328 (1999).
[12] K. H. Ahn and A. J. Millis, Phys. Rev. B **58**, 3697 (1998).
[13] V. Caignaert, F. Millange, M. Hervieu, E. Suard, and B. Raveau, Solid State Commun. **99**, 173 (1996).
[14] M. Tokunaga, N. Miura, Y. Tomioka, and Y. Tokura, Phys. Rev. B **57**, 5259 (1998).
[15] R. Pauthenet and C. Veyret, J. Phys. (Paris) **31**, 65 (1970).
[16] S. Y. Wu, C. M. Kuo, H. Y. Wang, W. H. Li, K. C. Lee, J. W. Lynn, and R. S. Liu, J. Appl. Phys. **87**, 5822 (2000).
[17] A. Munoz, J. A. Alonso, M. J. Martinez-Lope, J. L. Garcia-Munoz, and M. T. Fernandez-Diaz, J. Phys.: Condens. Matter **12**, 1361 (2000).
[18] S. Jandl, S. N. Barilo, S. V. Shiryaev, A. A. Mukhin, V. Yu Ivanov, and A. M. Balbashov, J. Magn. Magn. Mater. **264/1**, 36 (2003).
[19] M. Paraskevopoulos, F. Mayr, C. Hartinger, A. Pimenov, J. Hemberger, P. Lunkenheimer, A. Loidl, A. A. Mukhin, V. Yu. Ivanov, and A. M. Balbashov J. Magn. Magn. Mater. **211**, 118 (2000).
[20] Y. Tokura and Y. Tomioka, J. Magn. Magn. Mater. **200**, 1 (1999).
[21] I. O. Troyanchuk, V. A. Khomchenko, G. M. Chobot, A. I. Kurbakov, A. N. Vasil'ev, V. V. Eremenko, V. A. Sirenko, M. Yu Shvedun, H. Szymczak, and R. Szymczak, J. Phys.: Condens. Matter **15**, 8865 (2003).
[22] S. Jandl, P. Richard, V. Nekvasil, D. I. Zhigunov, S. N. Barilo, and S. V. Shiryaev, Physica C **314**, 189 (1999).
[23] G. Riou, S. Jandl, M. Poirier, V. Nekvasil, M. Divis, P. Fournier, R. L. Greene, D. I. Zhigunov, and S. N. Barilo, Eur. Phys. J. B **23**, 179 (2001).
[24] D. Barba, S. Jandl, V. Nekvasil, M. Marysko, J. Jurek, M. Divid, and T. Wolf, Phys. Rev. B **69**, 024528 (2004).
[25] G. Riou, S. Jandl, M. Poirier, V. Nekvasil, M. Marysko, J. Fabry, K. Jurek, M. Divis, J. Holsa, I. M. Sutjahja, A. A. Menovsky, S. N. Barilo, S. V. Shiryaev, and L. N. Kurnevich, Phys. Rev. B **66**, 224508 (2002).
[26] G. Riou, P. Richard, S. Jandl, M. Poirier, P. Fournier, V. Nekvasil, S. N. Barilo, and L. A. Kurnevich,, Phys. Rev. B **69**, 024511 (2004).
[27] P. Richard, G. Riou, I. Hetel, S. Jandl, M. Poirier, and P. Fournier, Phys. Rev. B **70**, 064513 (2004).
[28] A. A. Mukhin, V. Yu. Ivanov, V. D. Travkin, and A. M. Balbashov, J. Magn. Magn. Mater. **226–230**, 1139 (2001); Phys. Met. Metallogr. **91**, 194 (2001).
[29] S. Jandl, V. Nekvasil, M. Dicis, A. A. Mukhin, J. Hölsä, and M. L. Sadowski, Phys. Rev. B **71**, 024417 (2005).
[30] M. N. Iliev, M. V. Abrashev, V. N. Popov, and V. G. Hadjiev, Phys. Rev. B **67**, 212301 (2003).
[31] R. T. Harley, in *Spectroscopy of Solids Containing Rare Earth Ions*, edited by A. A. Kaplyanskii and R. M. Macfarlane (Elsevier, New York, 1987).

[32] A. M. Balbashov, S. G. Karabashev, Ya. M. Mukovskiy, and S. A. Zverkov, J. Cryst. Growth **167**, 365 (1996).
[33] M. N. Iliev, M. V. Abrashev, H. G. Lee, V. N. Popov, Y. Y. Sun, C. Thomsen, R. L. Meng, and C. W. Chu, Phys. Rev. B **57**, 2872 (1998).
[34] M. N. Iliev and M. V. Abrashev, J. Raman Spectrosc. **32**, 805 (2000).
[35] P. Björnsson, M. Rübhausen, J. Bäckström, M. Käll, S. Eriksson, J. Eriksen, and L. Börjesson, Phys. Rev. B **61**, 1193 (2000).
[36] M. V. Abrashev, A. P. Litvinchuk, M. N. Iliev, R. L. Meng, V. N. Popov, V. G. Ivanov, R. A. Chakalov, and C. Thomsen, Phys. Rev. B **59**, 4146 (1999).
[37] V. B. Podobedov, A. Weber, D. B. Romero, J. P. Rice, and H. D. Drew, Solid State Commun. **105**, 589 (1998).
[38] A. S. Barker and A. J. Sievers, Rev. Mod. Phys. **47**, Suppl. 2, 1 (1975).
[39] H. Y. Hwang, S. W. Cheong, P. G. Radaelli, M. Marezio, and B. Batlogg, Phys. Rev. Lett. **75**, 914 (1995).
[40] M. Pattabiraman, P. Murugaraj, G. Rangarajan, C. Dimitropoulos, J.-Ph. Ansermet, G. Papavassiliou, G. Balakrishnan, D. McK. Paul, and M. R. Lees, Phys. Rev. B **66**, 224415 (2002).
[41] E. Granado, A. Garcia, J. A. Sanjurjo, C. Rettori, I. Torriani, F. Prado, R. Sanchez, A. Caneiro, and S. B. Oseroff, Phys. Rev. B **60**, 11879 (1999).
[42] J. Bala, A. M. Oles, and G. A. Sawatzky, Phys. Rev. B **65**, 184414 (2002).
[43] J. van den Brink, Phys. Rev. Lett. **87**, 217202 (2001).
[44] Y. Murakami, J. P. Hill, D. Gibbs, M. Blume, I. Koyama, M. Tanaka, H. Kawata, T. Arima, Y. Tokura, K. Hirota, and Y. Endoh, Phys. Rev. Lett. **81**, 582 (1998)